# Numerical Studies of Fluid Leakage from a Geologic Disposal Reservoir for $CO_2$ Show Self-Limiting Feedback between Fluid Flow and Heat Transfer

Karsten Pruess
Earth Sciences Division, Lawrence Berkeley National Laboratory
Berkeley, CA 94720

**Abstract**

Leakage of $CO_2$ from a hypothetical geologic storage reservoir along an idealized fault zone has been simulated, including transitions between supercritical, liquid, and gaseous $CO_2$. We find strong non-isothermal effects due to boiling and Joule-Thomson cooling of expanding $CO_2$. Leakage fluxes are limited by limitations in conductive heat transfer to the fault zone. The interplay between multiphase flow and heat transfer effects produces non-monotonic leakage behavior.

## 1. Introduction

Storage of greenhouse gases, primarily $CO_2$, in geologic formations has been proposed as a possible means by which atmospheric emissions of such gases may be reduced (Bachu et al., 1994; Orr, 2004). The amount of $CO_2$ emitted from fossil-fueled power plants is very large, of the order of 30,000 tonnes per day (10 million tonnes per year) for a large 1,000 MW coal-fired plant (Hitchon, 1996). In order to make a significant impact on reducing emissions, very large amounts of $CO_2$ would have to be injected into subsurface formations, resulting in $CO_2$ disposal plumes with linear dimensions of order 10 km or more (Pruess et al., 2003). It appears inevitable, then, that such plumes will encounter imperfections in caprocks, such as fracture zones or faults, that would allow $CO_2$ to leak from the primary storage reservoir. At typical subsurface conditions of temperature and pressure, $CO_2$ is always less dense than aqueous fluids, and therefore buoyancy forces will tend to drive $CO_2$ upward, towards the land surface, whenever adequate (sub-)vertical permeability is available. Upward migration of $CO_2$ could also occur along wells, including pre-existing wells in sedimentary basins where oil and gas exploration and production may have been conducted (Celia et al., 2004), or along wells drilled as part of a $CO_2$ storage operation.

There are several concerns with leakage of $CO_2$ from man-made storage reservoirs, the most immediate one being to keep $CO_2$ away from the atmosphere, which is the reason for injecting it underground in the first place. A number of studies suggest that leakage rates sufficiently small as to not defeat the objective of geologic storage should be easily attainable (Pacala, 2003; Hepple and Benson, 2003). Additional concerns include acidification of groundwater from ingress of $CO_2$, and asphyxiation hazard should $CO_2$ be released at the land surface (Oldenburg and Unger, 2003;

Oldenburg and Lewicki, 2004). Another concern is whether it may be possible for a $CO_2$ leak to be self-enhancing, in such a way as to give rise to a runaway discharge at the land surface with potentially serious consequences. $CO_2$ has physical properties that suggest that such a possibility should be taken seriously, including lower density, and much lower viscosity and higher compressibility than aqueous fluids. As $CO_2$ migrates upward along a localized permeable pathway, fluid mobility and flow rates may increase when resident aqueous fluids are being displaced, and a huge expansion in volume will occur upon decompression. An eruptive release of $CO_2$ that gave rise to many human and livestock fatalities occurred in 1986 at Lake Nyos in Cameroon (Tazieff, 1989). Non-condensible gases, chiefly $CO_2$, are known to have played an ancillary role in many hydrothermal eruptions (Browne and Lawless, 2001). Volcanologists have suggested the possibility of "pneumatic eruptions" for natural systems, which would be driven primarily by the compressive energy that is stored in underground accumulations of high-pressure $CO_2$, with only minor contributions from thermal energy (Chivas et al., 1987; Allard et al., 1989; Giggenbach et al., 1991).

The mechanical energy of compression that would be stored in a $CO_2$ storage reservoir over the life time of a power plant is very large. The compression power (energy per unit time) required for underground storage of $CO_2$ can be estimated by considering a quasi-static displacement at constant pressure for representative *in situ* conditions at 1,000 m depth ($P \approx 100$ bar, $T \approx 36$ ˚C) with *in situ* density of approximately 700 kg/m$^3$. Power is defined as work per unit time, $N = dW/dt$, and substituting for compressible work $dW = PdV$, we have $N = PdV/dt = (P/\rho)dM/dt$. For a coal-fired power plant with 1,000 MW electric capacity, $CO_2$ emissions are approximately $3 \times 10^7$ kg per day, so that for the parameters assumed here we have $N \approx (10^7 \text{ Pa}/700 \text{ kg m}^{-3}) \times 3 \times 10^7 \text{ kg day}^{-1}/(86400 \text{ s day}^{-1}) \approx 5$ MW. The total compressive energy stored during a typical anticipated operating life of a $CO_2$ disposal project of 30 years then amounts to approximately $4.74 \times 10^{15}$ J, which is equivalent to the energy content of 1.1 megatonnes of TNT (1 megatonne of TNT corresponds to $4.184 \times 10^{15}$ J; Wikipedia, 2004). For a perspective on this number, note that a large prehistoric hydrothermal eruption at Rotokawa, New Zealand, which ejected approximately $10^7$ m$^3$ of material and generated a crater of more than 250 m diameter, has been estimated as having released an energy of $10^{14}$ J (Browne and Lawless, 2001). This is equivalent to 23.9 kilotonnes of TNT, similar to the atomic bomb that was dropped on Hiroshima. From these considerations it is clear that even a small fraction of the mechanical energy that would be stored in a geologic disposal system for $CO_2$, if released in localized fashion over a short period of time, could cause very substantial damage.

In order to assess risks associated with geologic storage of $CO_2$, and to identify favorable as well as unfavorable geologic conditions, and monitoring needs and opportunities, it is necessary

to develop a quantitative, mechanistic understanding of $CO_2$ leakage behavior. It is the purpose of this paper to present numerical modeling studies of hypothetical leakage systems, to begin the exploration of relevant flow mechanisms and behavior.

## 2. Thermodynamics of $CO_2$ Leakage

Let us consider the temperature and pressure conditions that would be encountered by bubbles of $CO_2$ migrating upward through permeable formations at rates so small that they would cause negligible disturbance of *in situ* temperature and pressure conditions. In "normal" crustal environments, we have a typical geothermal (temperature) gradient of $|\nabla T| \approx 30$ ˚C/km, while fluid pressures increase with depth according to a typical hydrostatic gradient of $|\nabla P| \approx 100$ bar/km. The resulting temperature and pressure conditions are shown in Fig. 1 for two different values of average land surface temperature, along with the saturation (liquid-gas coexistence) line for $CO_2$ (Bachu, 2003; Pruess, 2005). Both profiles are seen to pass in the vicinity of the critical point of $CO_2$ ($T_{crit}$ = 31.04 ˚C, $P_{crit}$ = 73.82 bar), and the one for a land surface temperature $T_{ls}$ = 5 ˚C actually intersects the $CO_2$ saturation line. In the latter case, a bubble of $CO_2$ slowly rising from depth will remain in liquid conditions until it reaches the saturation line at a pressure of 63 bar, corresponding to a depth below the water table of approximately 630 m. At this point the liquid $CO_2$ will boil into gas, which is accompanied by a large increase in volume and a decrease in viscosity. If this process occurs at a finite rate, it will cause formation temperatures to decline as latent heat is absorbed by the phase change process. An additional temperature decline will occur from Joule-Thomson cooling, as the gaseous $CO_2$ depressurizes and expands when it migrates to shallower horizons. From these considerations we expect that upward migration of $CO_2$ may be accompanied by significant non-isothermal effects, and previous simulation studies have shown this to be the case (Pruess, 2004b, 2005).

Numerical simulation of such leakage processes requires an accurate representation of the thermophysical properties of the fluids involved, including fluid density, viscosity, and specific enthalpy, along with mutual dissolution of water and $CO_2$, and heat of dissolution and vaporization effects. It also requires a recognition and treatment of the different fluid phase conditions. In a water-$CO_2$ system at temperatures above the freezing point we may have three different phases, a- aqueous, l - liquid, and g - gas, which may occur in seven different combinations (Fig. 2). In addition we need to model transitions between super- and sub-critical fluids, and we need constitutive relations (relative permeabilities and capillary pressures) for the 3-phase system aqueous–liquid–gas. We have developed simulation capabilities in the framework of the multiphase, non-isothermal flow simulator TOUGH2 (Pruess, 2004a) that meet all these requirements (Pruess,

2004b, 2005). We now proceed to discuss geometric and hydrogeologic specifications of an idealized leakage system for which numerical simulations were conducted.

## 3. Idealized Fault (Fracture) Zone

Fig. 3 shows an idealized fault zone that is modeled as a homogeneous permeable medium of 1,000 m vertical extent, 200 m width, and 1 m thickness, sandwiched between country rock of permeability so low as to be negligible on the time scales to be considered. The flow system is two-dimensional, but as will be seen important heat transfer effects may take place in the third dimension, perpendicular to the fault plane. These effects are taken into account by modeling the impermeable rock adjacent to the fault zone as semi-infinite conductive half spaces, and using the approximate semi-analytical method of Vinsome and Westerveld (1980) to represent transient heat conduction in these regions (Pruess, 2005). The flow system is prepared with geothermal/hydrostatic initial conditions as shown in Fig. 1, and $CO_2$ leakage is initiated by applying $CO_2$ at a pressure of 80 bar over a 6 m wide section of the fault at 710 m depth, where initial hydrostatic pressure is approximately 70.5 bar. Thus, we do not model the behavior of the primary $CO_2$ storage reservoir, nor do we address the question of how $CO_2$ will actually migrate from the storage reservoir to the fault. We simply assume that leakage from the primary storage reservoir will cause $CO_2$ to be present at a constant overpressure in a small subvolume of the fault zone, and we numerically model the subsequent evolution of the flow system. A depth of 710 m for introducing $CO_2$ into the fault zone was chosen so that fluid pressures would be near-critical, and expansion effects upon $CO_2$ decompression would be large. The left boundary of the fault zone is assumed "no flow" and may be interpreted as a symmetry boundary. Salinity effects were neglected in the study reported here, as were chemical interactions between rocks and fluids (Xu et al., 2004).

For the numerical simulation, we specify a horizontal discretization ranging from 2 m at the left boundary to 10 m at the right boundary, while a uniform discretization of 20 m is employed in the vertical direction. Other model parameters are given in Table 1. No information on relative permeabilities in the system water-$CO_2$ is currently available. We have employed a modified version of Stone's three-phase relative permeability functions (Stone, 1970), with parameters as commonly used for 3-phase flow problems involving a non-aqueous phase fluid (NAPL), such as liquid hydrocarbons or organic solvents, in the unsaturated zone. Water is considered the wetting phase, gaseous $CO_2$ non-wetting, with liquid $CO_2$ having intermediate wettability (playing the role of the NAPL). The modification of Stone's function employed here involves adjusting the liquid phase relative permeability in such a way that, for aqueous-liquid or aqueous-gas conditions with the same aqueous phase saturation $S_a$, we have $k_{rl}(1\text{-}S_a) = k_{rg}(1\text{-}S_a)$. Capillary pressures were neglected.

## 4. Results

After the $CO_2$ enters the fault zone, it partially dissolves in the aqueous phase, but most of it forms a separate, supercritical phase that is immiscible with water and displaces the resident aqueous phase. The $CO_2$-rich phase migrates upward, whereupon it decompresses and cools, inducing conductive heat transfer from the wall rocks. Temperatures decline and thermodynamic conditions reach the saturation line, with liquid $CO_2$ boiling into gas, even for warmer land surface conditions where the initial T,P-profile does not intersect the $CO_2$ saturation line. As there always is an aqueous phase present, the region with liquid-gas $CO_2$ conditions actually becomes a 3-phase zone, in which fluid mobility is strongly reduced by interference between the aqueous, liquid, and gas phases. As a consequence, $CO_2$ upflow is reduced locally in the three-phase zone, and an increasing fraction of upflowing $CO_2$ is diverted sideways to flow around that zone. This flow diversion reduces $CO_2$ fluxes and cooling rates in the 3-phase zone, and allows temperatures to recover by heat conduction from the wall rocks, causing liquid $CO_2$ to boil away. This will eventually cause thermodynamic conditions to go back to two-phase (aqueous-gas), with increased fluid mobility, whereupon $CO_2$ fluxes increase. The result is that we obtain quasi-periodic cycling of $CO_2$ fluxes, temperatures, and 3-phase conditions.

Figs. 4-7 present detailed results for $CO_2$ migration in a 1 m thick fault zone, for land surface conditions of $T_{ls}$ = 15 ˚C, $P_{ls}$ = 1.013 bar. Two snapshots of the $CO_2$ plume at different times are shown in Fig. 4, indicating that over time more of the upflowing $CO_2$ gets diverted sideways, away from the injection point. This is due to reduced fluid mobility in the 3-phase region, which initially forms above the injection point, and later broadens sideways, due to the lateral flow diversion and associated cooling effects (Fig. 5). Temperatures reach a minimum above the injection point near the top of the 3-phase zone, where boiling effects and associated heat loss are strongest (not shown). Fig. 6 shows that thermodynamic conditions get drawn towards the critical point and then along the $CO_2$ saturation line, which can be understood from the strong increase of $CO_2$ specific enthalpy $h$ upon decompression, with maximum values of $|\partial h/\partial P|_T$ occurring at the critical point and along the saturation line (Pruess, 2005). Over time, temperatures at the boiling front decline to low values (Fig. 6), and for the conditions specified in this simulation would eventually reach the freezing point of water, as well as conditions where $CO_2$-hydrates may form (Pruess, 2005). Our simulator currently has no provisions to deal with phase changes to water ice and hydrates, so that we must stop the simulation before they would occur.

Fig. 7 shows $CO_2$ fluxes at the land surface at two points, 1 and 175 m from the left boundary, respectively. It is seen that the fluxes go through quasi-periodic oscillations whose

period increases over time. It is interesting to note that the x = 1 m and x = 175 m fluxes are almost exactly out of phase. For comparison we performed another simulation in which fault zone temperatures were artificially held fixed at initial values by specifying very large specific heat for the rocks. This did not evolve any 3-phase conditions and showed a monotonic increase of leakage fluxes with time (curve marked "fixed temperature" in Fig. 7), indicating that it is limitations in conductive heat transfer that limit the growth of $CO_2$ fluxes in the non-isothermal case. The non-monotonic behavior of the leakage fluxes can be understood in terms of the evolution of 3-phase conditions and associated fluid mobility and temperature effects. Fig. 7 also shows the total 3-phase volume vs. time, demonstrating quasi-periodic variations that are in-phase with the x = 175 m fluxes, and out of phase with the x = 1 m fluxes. The interpretation of this observation is as follows. As the volume of the 3-phase zone increases with time, due to temperature decline from Joule-Thomson cooling and associated condensation effects in the region with gaseous $CO_2$, upflow through this zone is reduced due to reduced fluid mobility. This causes $CO_2$ fluxes above this zone (x = 1 m) to decline, while simultaneously causing sideways diversion of $CO_2$ upflow, with increased fluxes at x = 175 m.

We have explored $CO_2$ migration behavior for a range of parameter variations and in most cases observe a non-monotonic evolution of leakage fluxes, indicating that this type of behavior will occur not just for a special, fortuitous combination of problem parameters. As an example, Fig. 8 shows quasi-periodic variations seen in a simulation for a low-rate leak, induced by applying $CO_2$ at a small overpressure of approximately 1 bar at the bottom of the fault zone (1,000 m depth). Our limited sensitivity studies indicate that a tendency towards quasi-periodic variations is pervasive, and is attributable to the different time constants for phase change and multiphase flow in the fault plane, as compared to characteristic times for heat conduction.

## 5. Concluding Remarks

Our simulations of migration of free-phase $CO_2$ in a vertical fault show strong cooling effects from boiling of liquid $CO_2$, and from expansion of gaseous $CO_2$. The system evolution is dominated by thermodynamics of near-critical conditions, liquid-gas phase change, and decompression of gas. Fluid dynamics mechanisms that would increase $CO_2$ leakage rates over time, such as increases in buoyancy force and fluid mobility (viscosity and relative permeability effects), are countered by effects arising from limitations in the rate of conductive heat transfer. The strong feedback between fluid flow and heat transfer tends to limit $CO_2$ fluxes, gives rise to quasi-periodic variations in flow rates, and makes it difficult to envision scenarios in which leakage of $CO_2$ as a free phase could develop a self-enhancing runaway discharge at the land surface. However, the evidence produced by our simulation studies is not sufficient to completely dismiss

the possibility of a pneumatic eruption of $CO_2$, and more comprehensive studies are needed to ascertain the manner in which $CO_2$ may be released at the land surface. Such studies should incorporate more realistic models for leakage paths, including systems with regional groundwater flow and multiple barriers, and formation of secondary accumulations of $CO_2$.

Heat transfer limitations for $CO_2$ leakage may be much less severe if the $CO_2$ would migrate to shallower horizons not as a free phase but dissolved in water. $CO_2$ leaking from the primary storage reservoir as aqueous solute may produce secondary accumulations of dissolved $CO_2$ at shallower horizons, which may be capable of generating a self-enhancing release following exsolution of the $CO_2$ and formation of a free phase. Outgassing of $CO_2$ in volcanic areas and the role of non-condensible gases in hydrothermal eruptions may provide useful guidance and natural analogs for constraining leakage behavior from man-made $CO_2$ storage reservoirs, and for identifying favorable as well as unfavorable conditions for $CO_2$ containment (Chiodini et al., 2004; Shipton et al., 2004, 2005).

**Acknowledgement**

The author is grateful to John Apps and Curt Oldenburg for their reviews and helpful suggestions. This work was supported by the Director, Office of Science, Office of Basic Energy Sciences of the U.S. Department of Energy under Contract No. DE-AC03-76SF00098.

**References**

Allard, P., Dajlevic, D. and Delarue, C. Origin of Carbon Dioxide Emanation from the 1979 Dieng Eruption, Indonesia: Implications for the Origin of the 1986 Nyos Catastrophe. *Journal of Volcanology and Geothermal Research,* v. 39, pp. 195-206, 1989.

Bachu, S. Screening and Ranking of Sedimentary Basins for Sequestration of CO2 in Geological Media in Response to Climate Change, *Env. Geol.,* Vol. 44, pp. 277–289, DOI 10.1007/s00254-003-0762-9, 2003.

Bachu, S., Gunter, W.D. and E.H. Perkins. Aquifer Disposal of CO2: Hydrodynamic and Mineral Trapping. *Energy Convers. Mgmt.,* Vol. 35, pp. 269 - 279, 1994.

Browne, P.R.L. and J.V. Lawless. Characteristics of Hydrothermal Eruptions, with Examples from New Zealand and Elsewhere, *Earth-Scienc Rev.,* Vol. 52, pp. 299–331, 2001.

Celia, M., S. Bachu, J.M. Nordbotten, S.E. Gasda and H.K. Dahle. Quantitative Estimation of CO2 Leakage from Geological Storage: Analytical Models, Numerical Models, and Data Needs, paper 228, presented at 7th International Conference on Greenhouse Gas Control Technologies. Vancouver, Canada. September 5-9, 2004.

Chiodini, G., C. Cardellini, A. Amato, E. Boschi, S. Caliro, F. Frondini and G. Ventura. Carbon Dioxide Degassing and Seismogenesis in Central and Southern Italy, *Geophys. Res. Let.,* Vol. 31, L07615, doi: 10.1029/2004GL019480, 2004.

Chivas, A.R., I. Barnes, W.C. Evans, J.E. Lupton and J.O. Stone. Liquid Carbon Dioxide of Magmatic Origin and its Role in Volcanic Eruptions, *Nature,* Vol. 326, No. 6113, pp. 587 - 589, 9 April 1987.

Giggenbach, W.F., Y. Sano, and H.U. Schmincke. CO2-rich Gases from Lakes Nyos and Monoun, Cameroon; Lacher See, Germany; Dieng, Indonesia, and Mt. Gambier, Australia – Variations on a Common Theme, *J. Volcanol. Geotherm. Res.,* Vol. 45, pp. 311–323, 1991.

Hepple, R.P. and S. Benson. Implications of Surface Seepage on the Effectiveness of Geologic Storage of Carbon Dioxide as a Climate Change Mitigation Strategy, in: J. Gale and Y. Kaya (eds.), *Greenhouse Gas Control Technologies,* pp. 261–266, Elsevier Science, Ltd., Amsterdam, The Netherlands, 2003.

Hitchon, B. (ed.). *Aquifer Disposal of Carbon Dioxide,* Geoscience Publishing, Ltd., Sherwood Park, Alberta, Canada, 1996.

Oldenburg, C.M. and A.J.A. Unger. On Leakage and Seepage from Geologic Carbon Sequestration Sites: Unsaturated Zone Attenuation, *Vadose Zone Journal,* 2, 287–296, 2003.

Oldenburg, C.M. and J.L. Lewicki. Leakage and Seepage in the Near-Surface Environment: An Integrated Approach to Monitoring and Detection, paper 84, presented at 7th International Conference on Greenhouse Gas Control Technologies. Vancouver, Canada. September 5-9, 2004.

Orr, F.M.Jr. Storage of Carbon Dioxide in Geologic Formations, *J. Pet. Tech.,* pp. 90–97, September 2004.

Pacala, S.W. Global Constraints on Reservoir Leakage, in: J. Gale and Y. Kaya (eds.), *Greenhouse Gas Control Technologies,* pp. 267–272, Elsevier Science, Ltd., Amsterdam, The Netherlands, 2003.

Pruess, K. The TOUGH Codes—A Family of Simulation Tools for Multiphase Flow and Transport Processes in Permeable Media, *Vadose Zone J.,* Vol. 3, pp. 738 - 746, 2004a.

Pruess, K. Numerical Simulation of $CO_2$ Leakage from a Geologic Disposal Reservoir, Including Transitions from Super- to Sub-Critical Conditions, and Boiling of Liquid $CO_2$, *Soc. Pet. Eng. J.,* pp. 237 - 248, June 2004b.

Pruess, K. Numerical Simulations Show Potential for Strong Non-isothermal Effects during Fluid Leakage from a Geologic Disposal Reservoir for CO2, *Dynamics of Fluids and Transport in Fractured Rock,* Geophysical Monograph, American Geophysical Union, in press, 2005.

Pruess, K., T. Xu, J. Apps and J. García. Numerical Modeling of Aquifer Disposal of CO2, Paper SPE-83695, *SPE Journal,* pp. 49 - 60, 2003.

Shipton, Z.K., J.P. Evans, D. Kirschner, P.T. Kolesar, A.P. Williams and J. Heath. Analysis of CO2 Leakage through 'Low-permeability' Faults from Natural Reservoirs in the Colorado Plateau, East-central Utah, in: S.J. Baines and R.H. Worden (eds.), *Geological Storage of Carbon Dioxide,* Geological Society, London, Special Publications, Vol. 233, pp. 43–58, London, England, 2004.

Shipton, Z.K., J.P. Evans, B. Dockrill, J. Heath, A. Williams, D. Kirchner and P.T. Kolesar. Natural Leaking CO2–Charged Systems as Analogs for Failed Geologic Storage Reservoirs, in: D.C. Thomas and S.M. Benson (editors), *Carbon Dioxide Capture for Storage in Deep*

*Geologic Formations – Results from the CO2 Capture Project*, pp. 699–712, Elsevier, Amsterdam 2005.

Stone, H.L. Probability Model for Estimating Three-Phase Relative Permeability, *Trans. SPE of AIME*, 249, 214-218, 1970.

Tazieff, H. Mechanism of the Nyos Carbon Dioxide Disaster and of so-called Phreatic Steam Eruptions, *J. Volcanol. Geotherm. Res.*, Vol. 39, pp. 109 - 116, 1989.

Vinsome, P.K.W. and J. Westerveld. A Simple Method for Predicting Cap and Base Rock Heat Losses in Thermal Reservoir Simulators, *J. Canadian Pet. Tech.*, 19 (3), 87–90, July-September 1980.

Wikipedia: http://en.wikipedia.org/wiki/Megaton, accessed 6 December 2004.

Xu, T, J.A. Apps, and K. Pruess. Numerical Simulation of CO2 Disposal by Mineral Trapping in Deep Aquifers, *Applied Geochemistry*, Vol. 19, Issue 6, pp. 917-936, June 2004.

Table 1. Parameters for fault zone model of $CO_2$ leak.

| | |
|---|---|
| Permeability | $k = 10^{-12}$ m$^2$ |
| Porosity | $\phi = 0.35$ |
| Pore compressibility | $c = 4.5 \times 10^{-10}$ Pa$^{-1}$ |
| Relative permeability: modified* from Stone's first 3-phase method (Stone, 1970) | |
| a - aqueous phase<br>$k_{ra} = \left[\frac{S_a - S_{ar}}{1 - S_{ar}}\right]^n$ | |
| irreducible aqueous phase saturation | $S_{ar} = 0.15$ |
| exponent | $n = 3$ |
| l - liquid phase<br>$k_{rl} = \left[\frac{\hat{S} - S_a}{\hat{S} - S_{ar}}\right]\left[\frac{1 - S_{ar} - S_{lr}}{1 - S_a - S_{lr}}\right] * \left[\frac{\left(\hat{S} - S_{ar}\right)\left(1 - S_a\right)}{\left(1 - S_{ar}\right)}\right]^n$ | $\hat{S} = 1 - S_g - S_{lr}$ |
| irreducible liquid phase saturation | $S_{lr} = 0.01$ |
| exponent | $n = 3$ |
| g - gas phase<br>$k_{rg} = \left[\frac{S_g - S_{gr}}{1 - S_{ar}}\right]^n$ | |
| irreducible gas phase saturation | $S_{gr} = 0.01$ |
| exponent | $n = 3$ |
| Capillary pressure | $P_{cgl} = 0$<br>$P_{cga} = 0$ |
| Thermal parameters | |
| formation thermal conductivity | 2.51 W/m ˚C |
| rock specific heat | 920 J/kg ˚C |
| rock grain density | 2600 kg/m$^3$ |

* see text

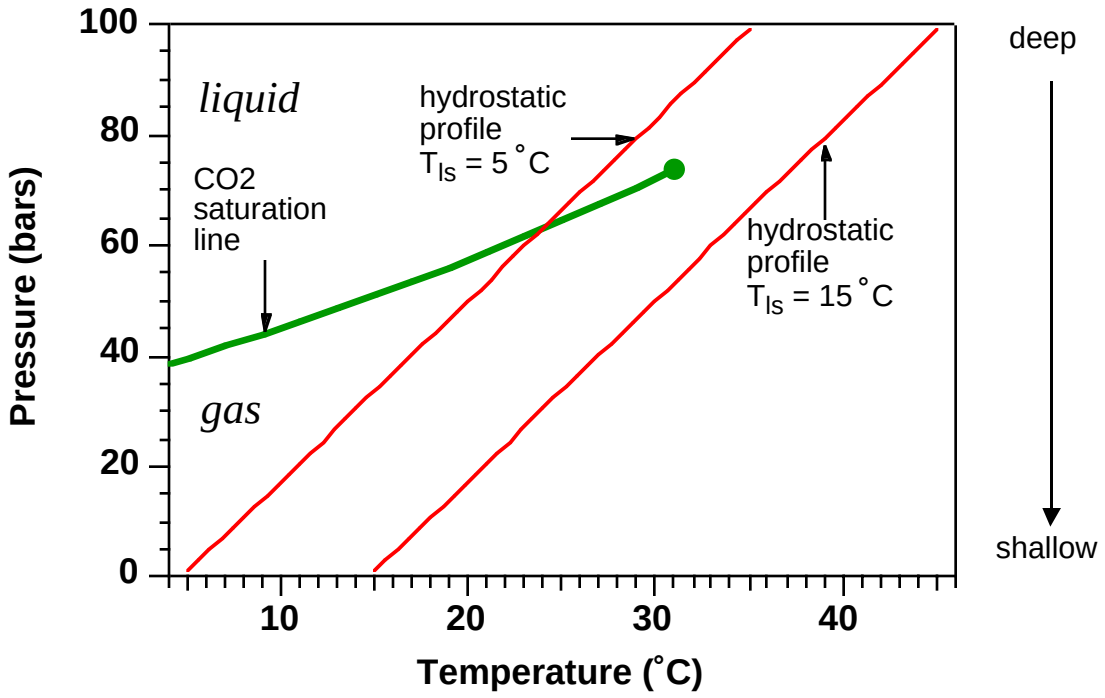


Figure 1. $CO_2$ saturation line and fluid pressure-temperature profiles for typical continental crust.

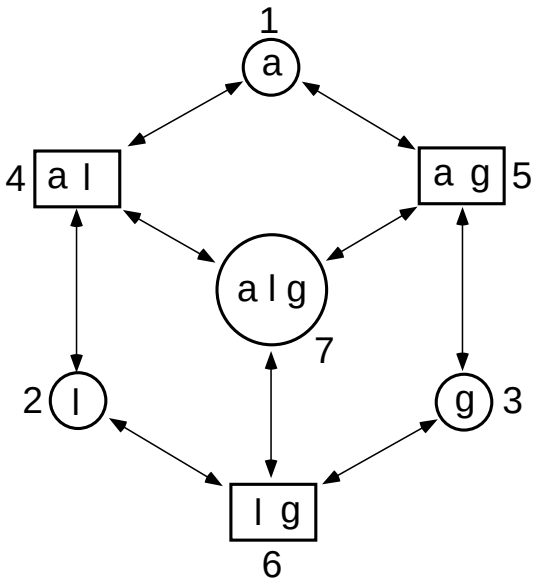


Figure 2. Possible phase conditions of water-$CO_2$ mixtures (a - aqueous, l - liquid $CO_2$, g - gaseous $CO_2$).

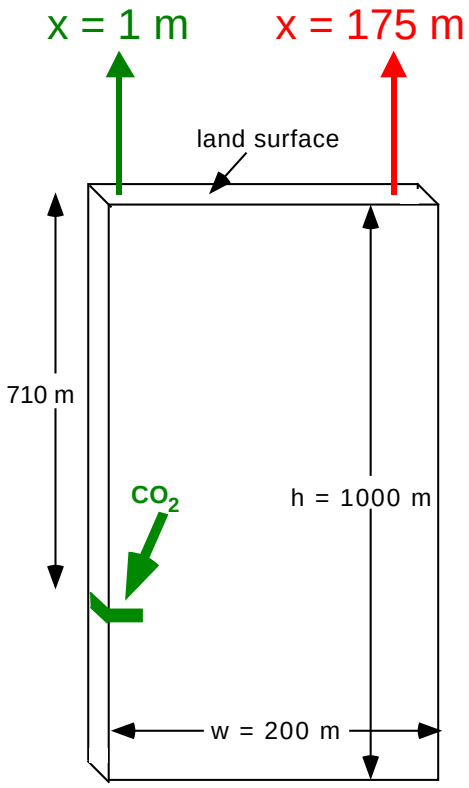


Figure 3. Schematic of idealized vertical fault zone for modeling $CO_2$ leakage. Land surface points at 1 m and 175 m distance from the left boundary are used to monitor leakage fluxes.

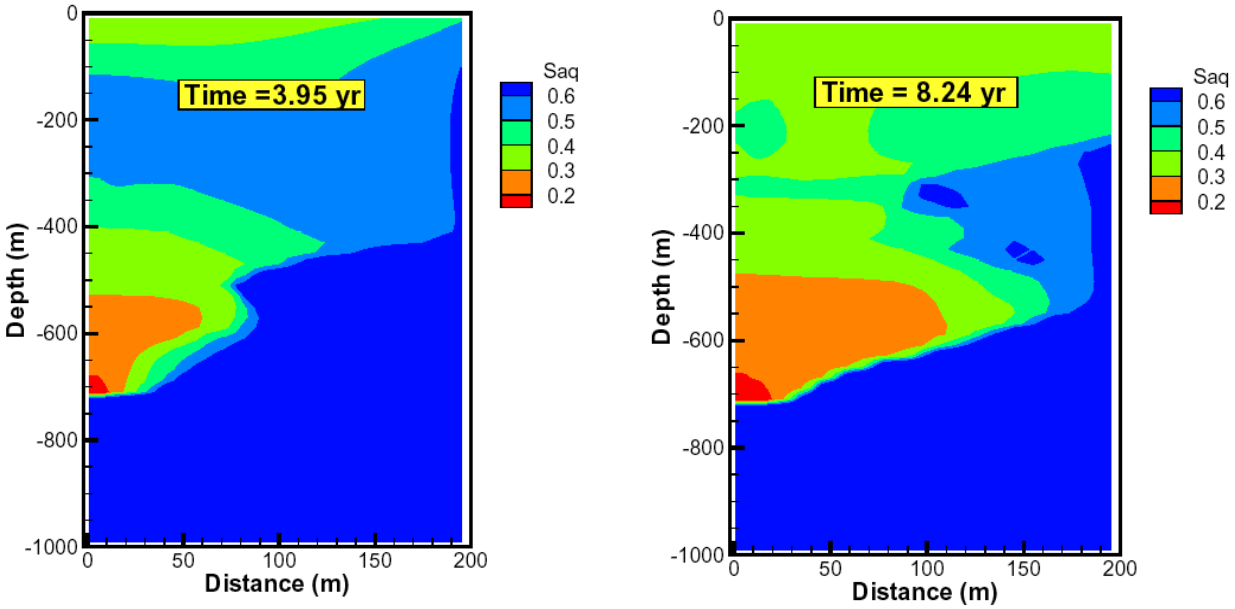


Figure 4. Simulated $CO_2$ plumes at two different times. The plumes include gaseous and liquid $CO_2$, and are shown by contour plots of aqueous phase saturation.

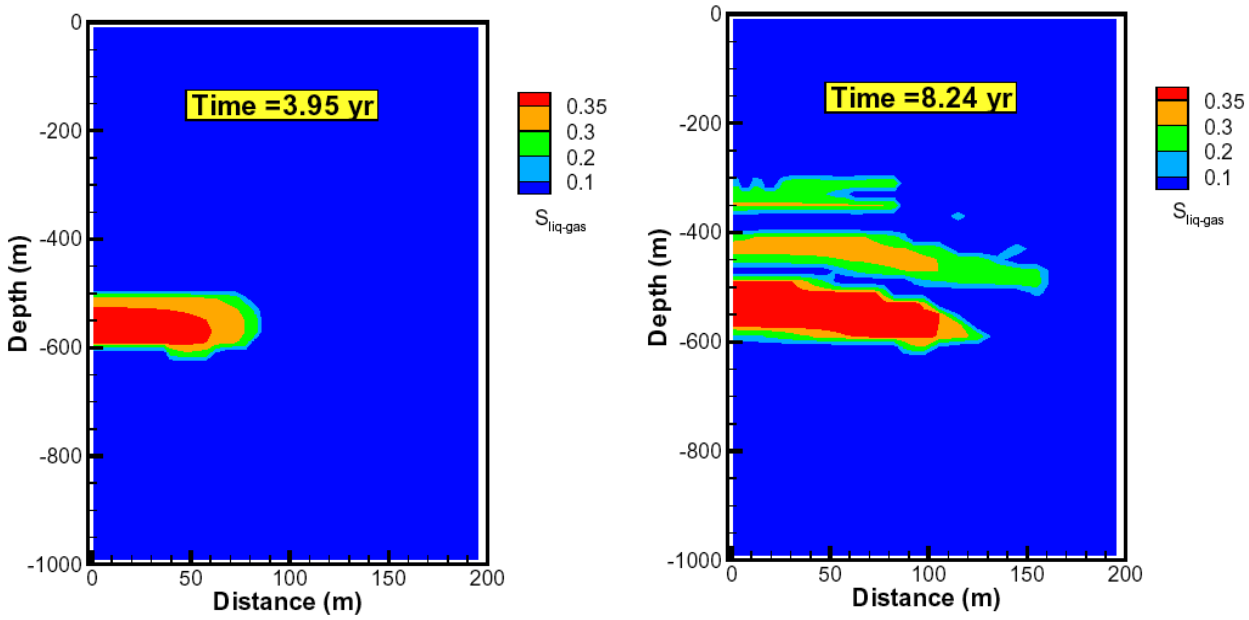


Figure 5. Simulated extent of three-phase regions at two different times. The parameter plotted is $S_{liq-gas} = \sqrt{S_{liq} \cdot S_{gas}}$, which is non-zero only for three-phase conditions.

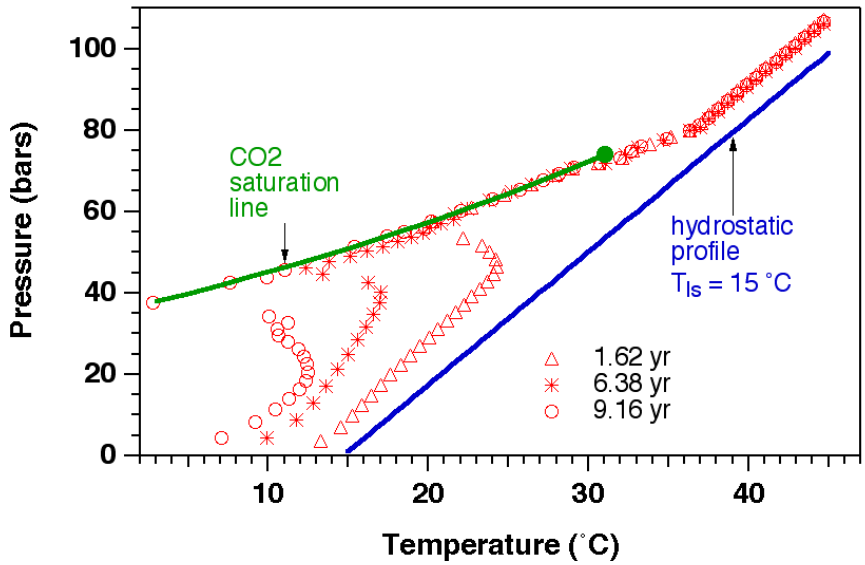


Figure 6. Pressure-temperature profiles in the leftmost column of grid blocks at different times.

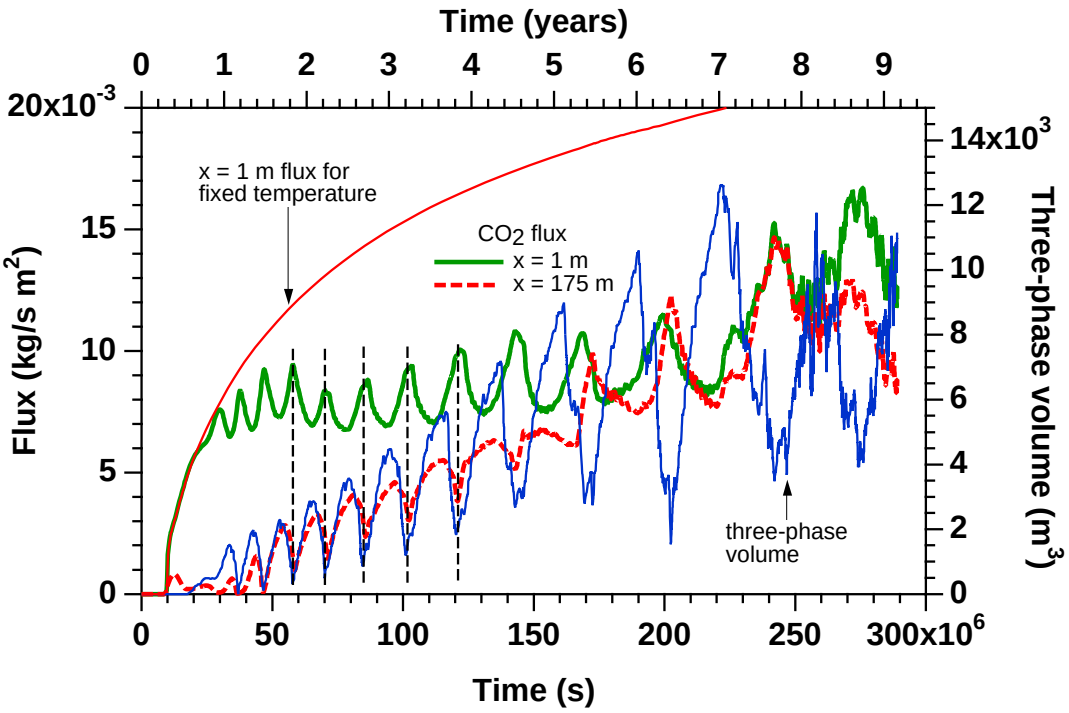


Figure 7. Temporal variation of $CO_2$ leakage fluxes at two different positions at the land surface. Total flow system volume with three-phase conditions is also shown. The vertical dashed lines are drawn to highlight the anticorrelation between leakage flux at x = 1 m on the one hand, and leakage flux at x = 175 m and three-phase volume on the other. The curve marked "fixed temperature" shows the simulated evolution of leakage fluxes in a system without heat transfer limitations.

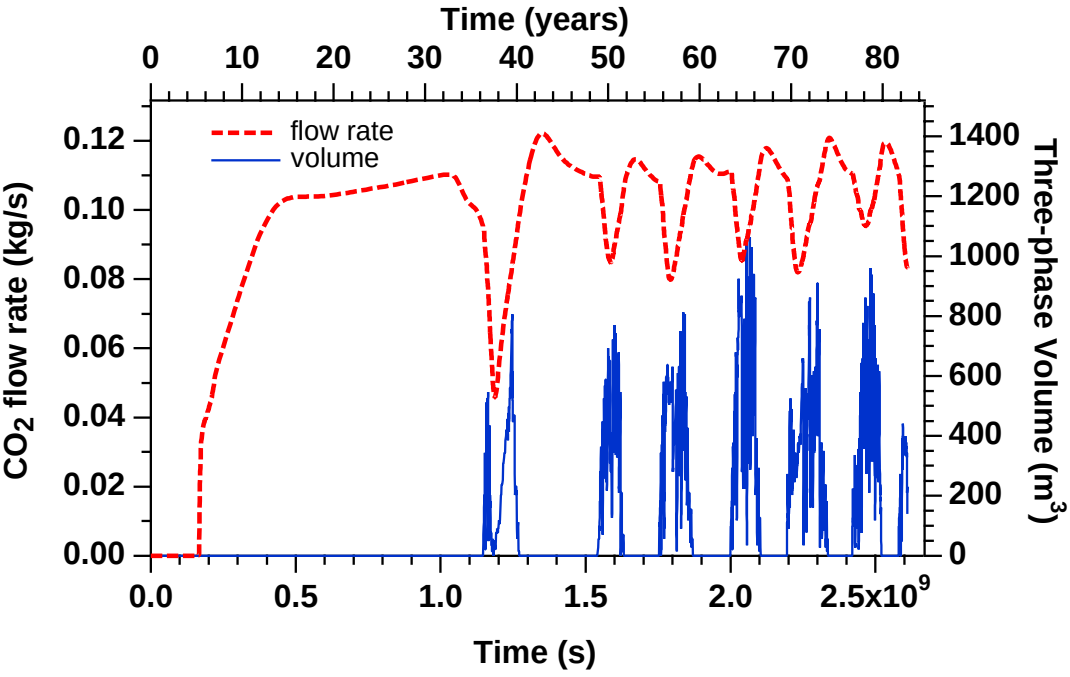


Figure 8. Total $CO_2$ leakage rate at the land surface and three-phase volume for a leak induced by small $CO_2$ overpressure of approximately 1 bar at the bottom of the fault zone.